

Design, Development, and Optimization of Spanlastics for Delivery of Rizatriptan Benzoate

Rajaa A. Dahash^{*1}   and Mowafaq M. Ghareeb²  

¹Ministry of Health, Baghdad, Iraq.

²Department of Pharmaceutics, College of Pharmacy, University of Baghdad, Baghdad, Iraq.

***Corresponding author**

Received 13/5/2024, Accepted 6 /10/2024, Published //



This work is licensed under a Creative Commons Attribution 4.0 International License.

Abstract

Spanlastics are nanovascular drug delivery systems that use surfactants, including hydrophilic and hydrophobic medicines. Spanlastics enhance the ability of medicines to enter the body and provide a continuous release over extended periods. These vesicles possess a high degree of elasticity and flexibility, enabling to improve the transportation of medications through different methods of administration. Rizatriptan Benzoate is prepared as spanlastics nanovesicles. Box-Behnken design was employed using Design-Expert[®] version 13.0.5.0 software (Stat-Ease, USA). The three independent variables were: (X1: Span[®]60 amount), (X2: Cremophor EL 40 amount), and (X3: sonication time). The dependent variables or responses were (Y1: Vesicle size), (Y2: PDI), and (Y3: Entrapment efficiency). The spanlastic formulations were developed using a response surface central composite design and formulated using an ethanol injection. The formulations were analyzed to identify the optimal formula with a minute particle size, lower PDI, and a high EE%. The optimized formula underwent additional analysis using zeta potential measurement, *in-vitro* release profile, Fourier Transform Infrared (FTIR) Analysis, Field Emission Scanning Electron Microscopy (FESEM), Differential Scanning Calorimetry Analysis (DSC), and X-ray Diffraction Analysis (XRD). The improved formulation exhibited a particle size of 84.98 ± 2.036 nm, a PDI of 0.1993 ± 0.045 and an EE% of $53.69 \pm 1.08\%$. There is a little discrepancy between the observed and predicted values. The zeta potential was -22.37 ± 0.74 . The optimum formula showed an appropriate release of $88.5 \pm 1.23\%$ over 6 hours. The compatibility analysis demonstrated that Rizatriptan Benzoate is compatible with the other excipients. Furthermore, the drug molecule was seen to exist in an amorphous condition within the spanlastic formula. Analysis of the vesicle shape revealed that it was nearly spherical. In summary, spanlastics have been considered as a possible delivery method for Rizatriptan Benzoate that might enhance its administration.

Keywords: Cremophor EL 40, Rizatriptan Benzoate, Nanovesicles, Span[®] 60, Spanlastics .

Introduction

Spanlastics are an innovative drug delivery device encapsulating medication in a bilayer within the core cavity. The term "Spanlastic" (a combination of "Span" and "Elastic") was coined in 2011. Spanlastics are viscoelastic vesicles formed by combining a vesicle builder with an edge activator (EA). EA interacts with the vesicle bilayer to alter its structural integrity, flexibility, and fluidic properties and can transport hydrophilic and hydrophobic medications. The hydrophilic pharmaceuticals are enclosed in the interior hydrophilic compartment, while the outside lipid layer encases the hydrophobic drugs⁽¹⁾. The formed spanlastics nanovesicles have garnered growing attention as a potential nanotechnology for medication delivery such as Rizatriptan benzoate (RNB). These vesicular carriers are a special type that may be used to transport drugs to specific sites in the body, such as the eyes, mouth, skin, nose, and nails. This ability is due to the specific properties of

spanlastic formulations; for example, edge activators enhance the flexibility of these systems, enabling the vesicles to pass through membrane barriers⁽²⁾. Ali M M et al. formulated intranasal spanlastic nanovesicles for rasagiline mesylate brain delivery⁽³⁾. The research employed the Design-Expert[®] program. A Box-Behnken design with three factors and three levels was utilized, employing response surface methodology, to investigate the impact of various variables on the chosen formulation. The formulation had been previously determined to have the highest desirability⁽⁴⁾. Migraine is a form of episodic neurological disorder distinguished by a pulsating headache that often affects one side of the head and is often accompanied by feelings of nausea and vomiting. The standard treatment of migraine typically consists of nonsteroidal anti-inflammatory drugs (NSAIDs), ergot alkaloids, and 5-HT receptor agonists (triptans). RNB, along with other triptans,

acts as an agonist on the 5HT1B/1D serotonin receptors and is regarded as the leading treatment for migraines. Nevertheless, the primary disadvantages of RNB oral formulations are the delayed initiation of effects and limited absorption into the bloodstream (40%) caused by the initial liver metabolism^(5,6). The objective of this work was to develop RNB as soft nano vesicular carriers, known as spanlastics, and examine the relationship between formulation parameters using Box-Behnken design with three independent variables were: (X1: Span® 60 amount), (X2: Cremophor EL40 amount), and (X3: sonication time) and the dependent variables as follows: Y1 represented vesicle size, Y2 represented PDI (polydispersity index), and Y3 represented entrapment efficiency. The ultimate goal was to create an appropriate spanlastics nanovesicular system for RNB that enhances the ability of medicines to enter the body.

Materials and Methods

Materials

RNB was supplied by Baoji Guokang Bio-Technology CO., LTD, China, and Cremophor EL was purchased from Hyper-Chem LTD CO, China. Span®60 was purchased from Xi'an Sonwu Biotech Co.Ltd, China Ethanol was purchased from Thomas Baker, India, and Deionized Water was purchased from Bainat al rafidain office, Iraq.

Methods

Rizatriptan Benzoate loaded spanlastics preparation

RNB spanlastic was prepared using the ethanol injection method. In summary, 10 ml of pure ethanol was utilized to dissolve RNB and Span® 60. The alcoholic solution was heated and then gradually injected into a preheated (70°C) water solution (10 ml) containing previously dissolved Cremophor EL 40 (an edge activator). The stirring process was prolonged by subjecting the mixture to magnetic stirring for 1 hour, ensuring all the ethanol had completely evaporated. The dispersion was subjected to probe sonication (QSonica, LLC, USA, 30% amplitude) at different times to enhance the formation of a finely dispersed and uniform mixture while preventing aggregate formation⁽⁷⁾. Ultimately, the formulations were stored in a refrigerator until they were examined.

In vitro characterization

Determination of vesicle size and PDI

The diluted formulation's vesicle size and polydispersity index (PDI) were measured using a Zetasizer from Malvern Instruments Ltd, United Kingdom. The measurements were performed at a temperature of 25±2 °C. To achieve precise measurements, the samples were diluted by a factor of 10 using distilled water before analysis⁽⁸⁾.

Determination of RNB entrapment efficiency (EE%)

The entrapment efficiency (EE %) of RNB using spanlastics vesicles was determined using ultrafiltration. RNB that was not captured was isolated from the spanlastics dispersion using the ultrafiltration method. Four mL of the spanlastics dispersion was added to the sample reservoir of the Amicon® Ultra-4 centrifugal filter (with a molecular weight cutoff of 10 kilo Daltons) from Merck Millipore Ltd. The mixture was then centrifuged at 6000 rpm using (Hettich centrifuge) for 30 minutes at room temperature. The removed filtrate from the spanlastics preparation contained untrapped RNB, which was not properly encapsulated within the spanlastics. To quantify the quantity of medication that was not trapped, the filtrate was examined using a UV spectrophotometer (model UV-1900I PC, Shimadzu, Kyoto, Japan) at a wavelength of 228 nm. The measurements were conducted three times. The EE percentage was calculated using equation 1^(9,10).

$$EE\% = \frac{\text{Amount of total drug} - \text{Amount of untrapped drug}}{\text{amount of total drug}} \times 100\% \quad (\text{Equation 1})$$

Studying the influence of different formulation variables using the Box-Behnken design

Box-Behnken design was employed using Design- Expert® version 13.0.5.0 software (Stat-Ease, USA). The three independent variables were: (X1: Span® amount), (X2: Cremophor EL 40 amount), and (X3: sonication time). The dependent variables or responses were (Y1: Vesicle size), (Y2: PDI), and (Y3: Entrapment efficiency), as shown in Table 1. Fifteen formulations with 3 center points of RNB spanlastics were prepared based on the above software, as shown in Table 2.

Table 1. Dependents and independent variables used in Box-Behnken design

Dependent variables	Levels
X1: Span® 60 amount	40 mg, 70 mg and 100 mg
X2: Cremophor EL 40	10 mg, 30 mg and 50 mg
X3: Sonication time	0 min, 4 min and 8 min
Y1: Vesicle size	Minimize
Y2: PDI	Minimize
Y3: Entrapment Efficiency	Maximize

Table 2. Design of RNB spanlastic formulations using Box-Behnken design software

Formula	Span® amount	Cremophor EL 40	Sonation time
1	70	50	8
2	70	50	0
3	70	30	4
4	70	10	0
5	70	10	8
6	70	30	4
7	40	50	4
8	70	30	4
9	40	10	4
10	100	30	8
11	100	10	4
12	40	30	0
13	100	30	0
14	100	50	4
15	40	30	8

Statistical Optimization of RNB Loaded Spanlastics Formulation

The selection of the optimum formula in this model was determined by minimizing the vesicle size and PDI and maximizing EE%. The actual responses (Y1, Y2, and Y3) were compared to the statistically predicted values, and the percentage relative error was determined using Equation 2 ⁽¹¹⁾. This was done to validate the improved method.

$$\% \text{ Relative error} = (\text{predicted value} - \text{observed value}) \times 100 / \text{predicted value} \quad (\text{Equation 2})$$

The efficacy of the revised nano formula was assessed using additional characterization experiments.

Characterization of the optimized formula

Zeta potential of the optimum RNB-loaded spanlastics

The net charges of the chosen RNB-loaded spanlastic nano vesicular formulations were determined by analyzing their zeta potentials. These zeta potentials can be utilized to assess the stability of the vesicular formulations. The diluted spanlastics dispersion was introduced into a disposable cuvette of a Zetasizer analyzer (Malvern Instruments, UK) equipped with software to detect electrophoretic mobility ⁽¹²⁾.

In-vitro release profile

The quantity of RNB liberated from the RNB solution and chosen spanlastics formula over a duration of six hours was determined utilizing the dialysis bag technique. Briefly, a certain spanlastic dispersion volume, equivalent to 14.53 mg RNB (14.53 mg of RNB equivalent to 10 mg rizatriptan), was selected from the available formulation and transferred into dialysis bags made of cellulose membrane with a molecular weight cutoff range of 8000-14000. The dialysis bags were placed in a paddle (type II- dissolving equipment) with 500 mL of freshly made phosphate buffer solution (pH =

7.4). The quantity of RNB was determined using a UV visible spectrometer with a detection wavelength of 225 nm ⁽¹³⁾.

Fourier Transform Infrared (FTIR) Analysis

The FTIR study was conducted by combining the optimal formula, physical combination, and drug alone with a tiny quantity of dry KBr powder. This mixture was then crushed into a clear disc, and spectra were collected in the region of 4000-500 cm⁻¹. The spectra were analyzed to confirm the absence of any interaction between the medicine and the excipients that might potentially occur throughout the procedure ⁽¹⁴⁾.

Field Emission Scanning Electron Microscopy (FESEM)

The surface morphology of the optimal spanlastics formula was analyzed using a field emission scanning electron microscope (FESEM). Following the dilution of one milliliter of nanodispersion with deionized water, a small amount of the diluted sample was applied to aluminum slabs and left to dry for a specific duration. The dry samples were coated with a thin coating of Au/Pd using a sputter coater. Subsequently, they were observed with a Field Emission Scanning Electron Microscope (FESEM) at different magnifications ⁽¹⁵⁾.

Transmission Electron Microscopy (TEM)

The morphological properties of the optimum drug nanosuspension were examined using a transmission electron microscope (TEM). The specimen was made by diluting a small amount of the chosen compound with distilled water and then allowing it to evaporate on a copper grid coated with carbon. Subsequently, it was analyzed using a transmission electron microscope (TEM) of the (Zeiss Supra 40vp, Germany). The transmission electron microscope (TEM) enabled researchers to observe and analyze the morphology of the

nanovesicles, as well as any other characteristics found in the sample ^(16,17).

Differential Scanning Calorimetry Analysis

The DSC method was utilized to evaluate the thermotropic characteristics and thermal behavior of the pure drug RNB, the RNB optimum lyophilized formula, and the physical mixture with a molar ratio of 1:1 between the drug and other excipients. A sample weighing approximately 5 mg was placed in aluminum pans and heated at a rate of 10 °C per minute. The temperature range during the experiment ranged from 25 °C to 300 °C ⁽¹⁸⁾.

X-ray Diffraction Analysis

X-ray powder diffraction tests were conducted to assess the degree of crystallinity of the medication in pure form and in RNB lyophilized and physical mixture of the optimum formula.

The measurements were conducted by placing the samples in glass sample holders. The scan range used was $2\theta = 5 - 80$. The operating voltage and current were set at 40 kV and 30 mA, respectively. Data was collected with a step width of 0.05° and a detector resolution in diffraction angle (2θ) between 5°C and 100°C at room temperature ⁽¹⁹⁾.

Results and Discussion

Effect of formulation variables on vesicle size and PDI

Predicting the factors that affect the action of pharmaceutical products is challenging. However, recent studies on the specific formulation have indicated that particle size is the most influential factor in determining the biological activity of each drug. This is because particle size controls the delivery of the drug to its intended target ⁽²⁰⁾. The spanlastics that were generated consisted of vesicles with a nano-sized range, with a mean ranging from 568.7 nm to 25.34 nm. An ANOVA study was conducted to assess the impact of independent variables on vesicle size. The results indicate that the span amount (X1), Cremophor EL 40 amount (X2), and sonication time (X3) have significant effects on vesicle size ($P < 0.0001$). Table 2. shows vesicle size, PDI, and EE% of the prepared RNB spanlastics formulas, as well as Figures 1, 2, and 3 display 3D charts illustrating the impact of independent parameters on vesicle size.

Table 2. Vesicles size, PDI, EE% of the prepared RNB spanlastics formula

Vesicle size* (nm)	PDI*	EE (%)*
39.2±1.7	0.2841±0.017	43.289±0.61
241.7±6.51	0.3264±0.21	54.211±1.25
129.3±5.12	0.2738±0.021	50.866±1.81
332.4±6.93	0.1477±0.014	68.267±1.03
180.7±2.64	0.145±0.011	56.031±0.61
169.7±5.51	0.1224±0.025	53.085±1.25
25.34±0.69	0.1582±0.019	36.297±0.59
151.5±5.51	0.3197±0.021	51.746±1.62
116.7±2.31	0.3141±0.022	52.051±3.03
380.5±5.52	0.1503±0.013	67.461±1.54
557.5±7.32	0.5774±0.029	66.223±0.64
84±4.11	0.2673±0.009	47.729±1.89
568.7±1.71	0.4798±0.022	70.589±1.59
291.4±4.73	0.2275±0.028	63.244±0.25
74.73±4.25	0.2059±0.31	43.741±1.31

*Results as mean ± SD, n=3

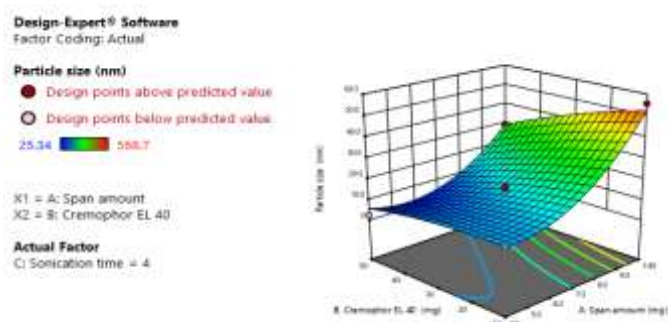


Figure 1. 3D-surface plots for the effect of the amount of Span®60 (A), Cremophor EL 40 (B) and sonication time (C) on the vesicle size of RNB spanlastics formulations ((A, B) effects on vesicle size).

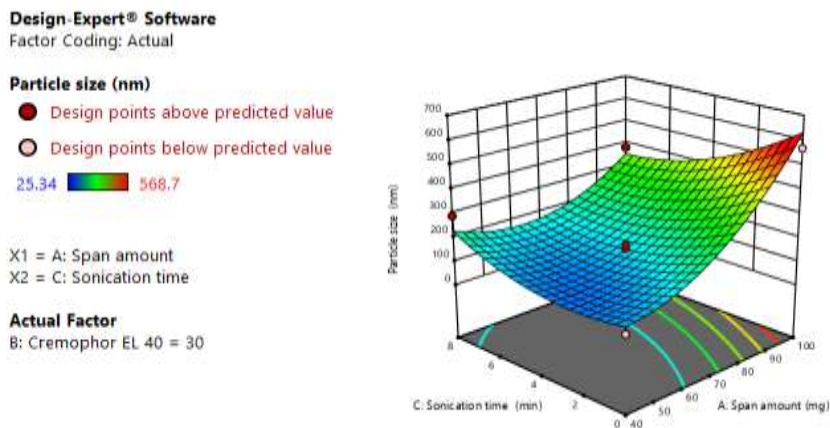


Figure 2. 3D-surface plots for the effect of the amount of Span®60 (A), Cremophor EL40 (B) and sonication time (C) on the vesicle size of RNB spanlastics formulations ((A, C) effects on vesicle size).

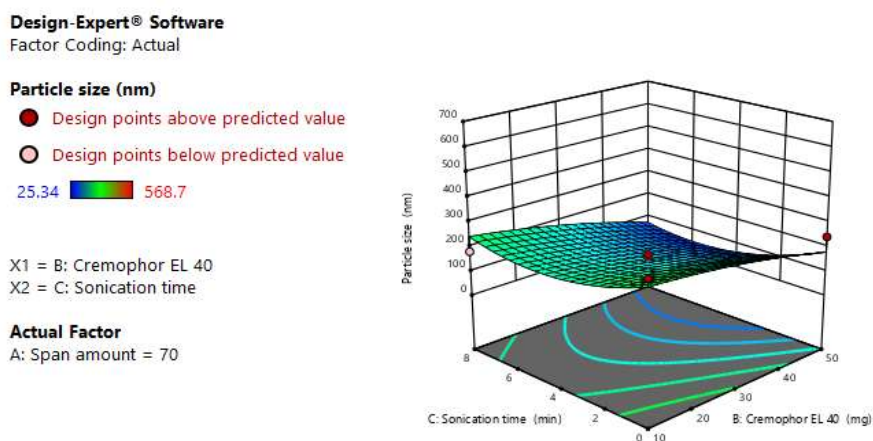


Figure 3. 3D-surface plots for the effect of the amount of Span®60 (A), Cremophor EL 40 (B) and sonication time (C) on the vesicle size of RNB spanlastics formulations ((B, C) effects on vesicle size).

The predicted R^2 value (0.8909) showed satisfactory concurrence with the adjusted R^2 value (0.9036), suggesting a strong correlation. The polynomial equation that demonstrates the relation between particle size and independent formulation factors is as follows: Particle size (Y_1) = +177.79 + 187.17 A – 73.71 B – 68.96 C + 84.57. Whereas A: Span® 60, B: Cremophor EL 40 amounts, and C: sonication time. It can be concluded that there is a substantial correlation between the amount of Span® 60 (X1) and the particle size ($p < 0.0001$). The results confirm the hypothesis that surfactants with longer alkyl chains produce vesicles with greater sizes⁽²¹⁾. According to Bhardwaj P. et al., Span® 60 produces the largest vesicles because it contains the longest alkyl chain without any unsaturation⁽²²⁾. The study found that increasing the amount of Cremophor EL 40 (X2) has a significant positive effect on vesicle size ($P < 0.05$). Increasing the

concentration of Cremophor EL 40 will result in a reduction in vesicle size since increased surfactant concentration promotes the formation of smaller droplets and is attributed to the enhanced migration of surfactant molecules from the oil phase to the aqueous phase, so effectively reducing the size of the drug particles⁽²³⁾. Regarding the impact of sonication time (X3) on vesicle size, it was observed that the efficiency of probe sonication in reducing vesicle size is significantly boosted by increasing the sonication period since ultrasound mechanical waves can cause cavitation or bubble formation in the vesicle membrane, the results demonstrated that longer sonication duration resulted in a decrease in the particle size. Increasing the duration of sonication resulted in the release of higher levels of sonication energy. This, in turn, facilitated the quick and uniform dispersion of the organic phase into nanovesicles^(24,25). An analysis of variance

(ANOVA) revealed that the effect of sonication time on vesicle size was statistically significant ($p < 0.05$).

Effects of Formulation Variables on PDI

The Polydispersity index (PDI) quantifies the degree of uniformity in the compositions. A formulation with a PDI (Y2) value near 0 implies a homogeneous population, whereas those with a PDI

value near 1 imply a heterogeneous system. The PDI values observed in our study ranged from 0.1224 to 0.5774, which suggests the presence of monodisperse systems ⁽²⁶⁾. The ANOVA investigation reveals no statistically significant impact of any independent factors on the values of PDI ($p < 0.05$). As depicted in figures (4,5 and 6).

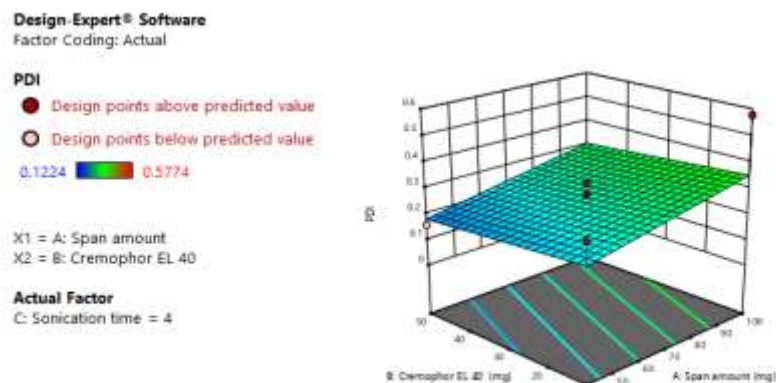


Figure 4. 3D-surface plots for the effect of the amount of Span®60 (A), Cremophor EL40 (B) and sonication time (C) on the PDI of RNB spanlastics formulations ((A, B) effects on PDI).

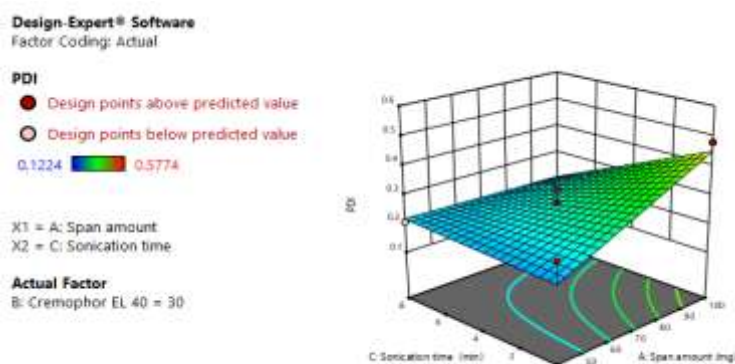


Figure 5. 3D-surface plots for the effect of the amount of Span®60 (A), Cremophor EL 40 (B) and sonication time (C) on the PDI of RNB spanlastics formulations ((A, C) effects on PDI).

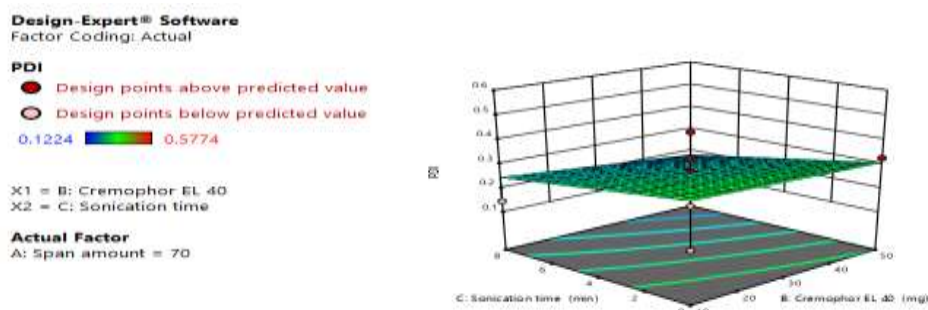


Figure 6. 3D-surface plots for the effect of the amount of Span®60 (A), Cremophor EL 40 (B) and sonication time (C) on the PDI of RNB spanlastics formulations ((B, C) effects on PDI).

Effects of formulation variables on entrapment efficiency

The entrapment efficiency of the produced spanlastics formulation ranged from 36.279 % to 70.589 %. The obtained results refer to the significant effect of variables on entrapment efficiency ($p < 0.0001$). The predicted R^2 (0.8895) was in a reasonable agreement with the adjusted R^2 (0.9076), indicating a good correlation. The polynomial equation that demonstrates the relation between EE% and independent formulation factors is as follows: Entrapment efficiency % (Y3) = $56.66 + 10.59 A - 6.07 B - 3.78 C$. There is a statistically significant increase ($p < 0.0001$) in plastics EE% as the amount of Span® 60 increases. The higher amount of Span® 60(X1) resulted in a substantial increase in EE% (Y2) at a p-value of less than 0.0001. This can be attributed to the solid state, hydrophobic character, and high phase transition

temperature (53°C) of Span® 60⁽²⁷⁾. The proportion of EE decreased dramatically ($p < 0.05$) as the amount of the Cremophor EL 40 (X2) increased; the smaller particles exhibited lower entrapment efficiency and enhancement of the hydrophilic properties of the nanovesicles since the HLB value of Cremophor EL 40 is 14, so resulting increase membrane fluidity and may lead to more creation of transitory hydrophilic holes inside the bilayer⁽²⁸⁾. The impact of size reduction procedures, specifically probe sonication, on drug leakage percentage is demonstrated. As the size reduces, the drug encapsulation efficiency (EE%) also falls, leading to higher rates of drug leakage relative to larger vesicles⁽²⁹⁾. Sonication time exhibited a significant impact ($p < 0.05$) on the percentage of entrapment of RNB within the vesicles. Figures 7,8 and 9 present 3D graphs depicting independent variables' influence on the EE%.

Design-Expert® Software
Factor Coding: Actual

EE (%)

● Design points above predicted value

○ Design points below predicted value

36.297 70.589

X1 = A: Span amount

X2 = B: Cremophor EL 40

Actual Factor

C: Sonication time = 4

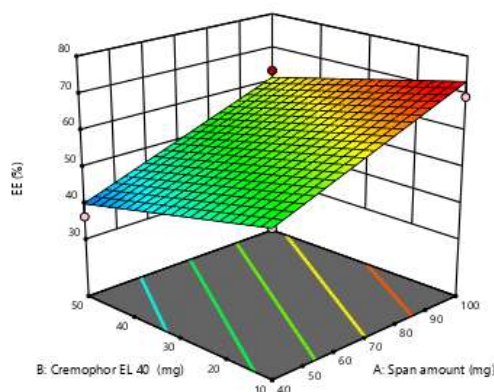


Figure 7. 3D-surface plots for the effect of the amount of Span®60 (A), Cremophor EL 40 (B) and sonication time (C) on the EE% of RNB spanlastics formulations ((A, B) effects on EE%).

Design-Expert® Software
Factor Coding: Actual

EE (%)

● Design points above predicted value

○ Design points below predicted value

36.297 70.589

X1 = A: Span amount

X2 = C: Sonication time

Actual Factor

B: Cremophor EL 40 = 30

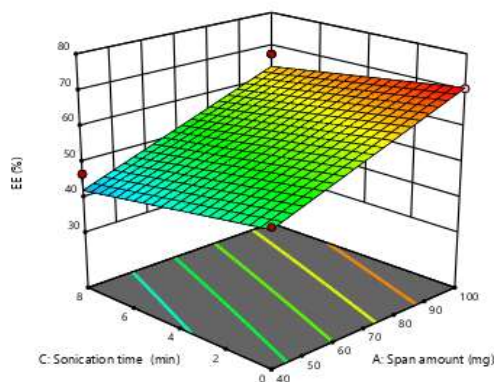


Figure 8. 3D-surface plots for the effect of the amount of Span®60 (A), Cremophor EL 40 (B) and sonication time (C) on the EE% of RNB spanlastics formulations ((A,C) effects on EE%).

Design-Expert® Software

Factor Coding: Actual

EE (%)

● Design points above predicted value

○ Design points below predicted value

36.297 70.589

X1 = B: Cremophor EL 40

X2 = C: Sonication time

Actual Factor

A: Span amount = 70

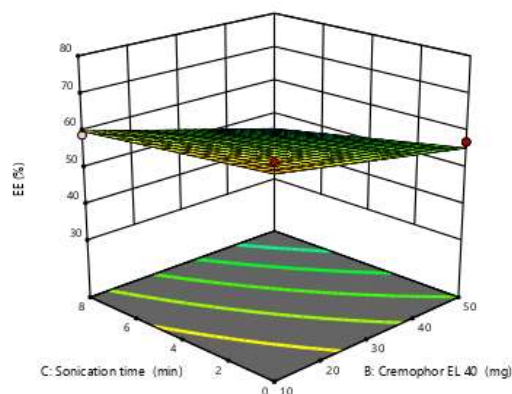


Figure 9. 3D-surface plots for the effect of the amount of Span®60 (A), Cremophor EL 40 (B) and sonication time (C) on the EE% of RNB spanlastics formulations ((B, C) effects on EE%).

Statistical optimization RNB loaded spanlastics formulation

The optimal formula was determined by integrating numerical and graphical optimization techniques with desirability criteria. The optimization study calculates a set of desirability functions for each response variable based on the selected criterion of either maximizing or minimizing. The estimated answers (Y1, Y2, and Y3) may be converted into a desirability value that increases in line with the attractiveness of the corresponding reaction using the desirability approach. The desirability value is a numerical measure ranging from zero to one. A formula with a desirability value of 1 is completely desired, whereas a grade of 0 indicates complete undesirability. The best formula has the greatest

desired value ⁽³⁰⁾. The optimized formula was selected by design with a higher desirability of 0.91 and contained 56.0152 mg of Span® 60 and 10 mg of Cremophor EL 40, with a sonication time of 8 minutes. It was predicted to have a vesicle size of 89.5765 nm, PDI 0.26664, and EE% of 54.0014. The optimized formula (actual value) was evaluated and compared to the predicted values (Figure 10). The optimized formula showed vesicles of 84.98 ± 2.036 nm size, PDI 0.1993 ± 0.045 , and EE% of $53.69 \pm 1.08\%$. The vesicle size exhibited a percent error of 0.051%, whereas the PDI displayed a percent error of 0.25%, and the EE% showed a 0.0057% percent of error. The small level of error suggests that the central composite model is sufficient and highly effective in optimizing predictions.

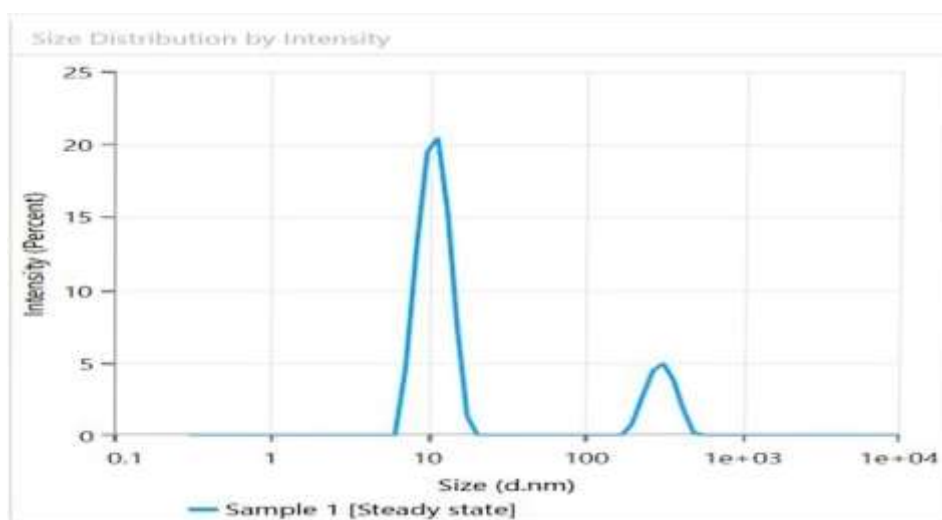


Figure 10. Vesicle size of the optimum formula (Actual value)

Characterization and Evaluation of Optimized Formulation

Zeta potential of the optimum RNB-loaded spanlastics

The optimal RNB-loaded plastic exhibited a zeta potential of $(-22.37 \pm 0.74 \text{ mV})$. Specifically, ZP is a factor for forecasting the stability of

nanoparticles over the long term; it represents the electric potential and surface charge of the nanoparticles during synthesis. Given the ZP values, Nanoparticles are unable to aggregate at larger concentrations due to the electrostatic repulsion of the attractive Vander Waals forces ⁽³¹⁾. Figures 11 demonstrate the optimum formula's zeta potential.

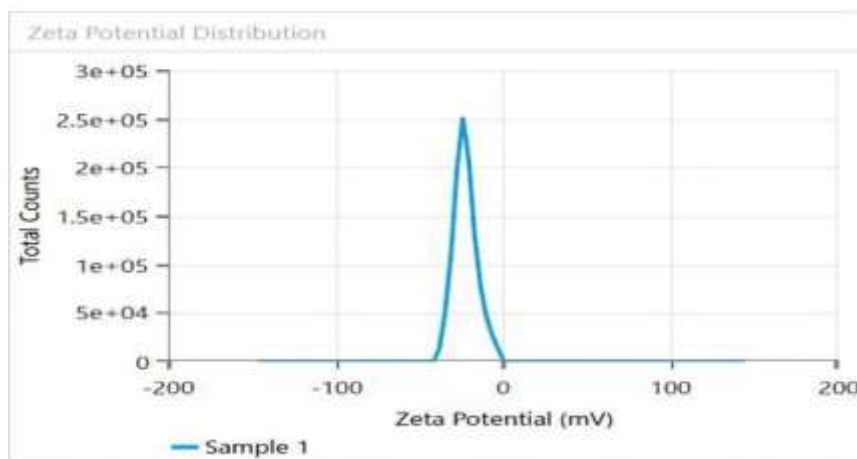


Figure 11. Zeta potential of the optimum formula

In-vitro release profile

The spanlastics optimum formula showed less drug release ($88.50 \pm 1.23\%$) compared to pure drug solution ($90.69 \pm 2.03\%$) at 6 h. The lower percentage of RNB released from the optimum formula, compared to the pure drug solution, may be due to RNB being entrapped in the lipophilic region of the Span® 60 bilayers, as well as the long alkyl chain length of Span® 60 along with the presence of Cremophor EL 40, the combination results in the formation of a high-order semisolid state and impermeable bilayer causing RNB to be released

more slowly from spanlastics than from the pure RNB solution, a different explanation for the drug's enhanced release is the inclusion of a surfactant, which functions as an edge activator or bilayer softening agent responsible for deformability and softness of the spanlastics leading to a better release from the vesicles ^(31,32). ANOVA analysis revealed a significant decrease in the release profile ($p < 0.05$) of the RNB spanlastic formula compared to the corresponding drug solution. Figure 12 represents *in-vitro* drug release (%) of RNB solution and RNB optimum in phosphate buffer solution at pH 7.4 at 37°C.

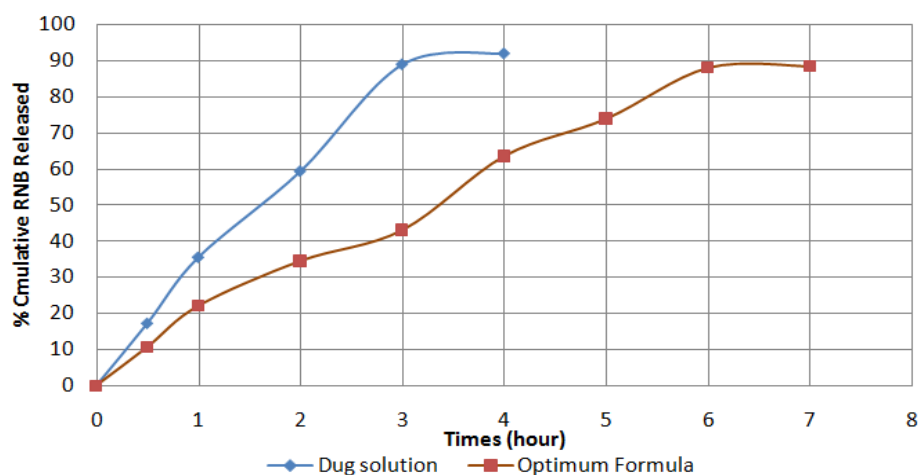


Figure 12. *In vitro* drug release (%) of RNB solution and RNB optimum in phosphate buffer solution at pH 7.4 at 37 °C

Fourier Transform Infrared (FTIR) Analysis

FTIR spectroscopic examination is valuable for determining the compatibility of medicine with different excipients. Furthermore, the FTIR analysis is an effective technique for examining any

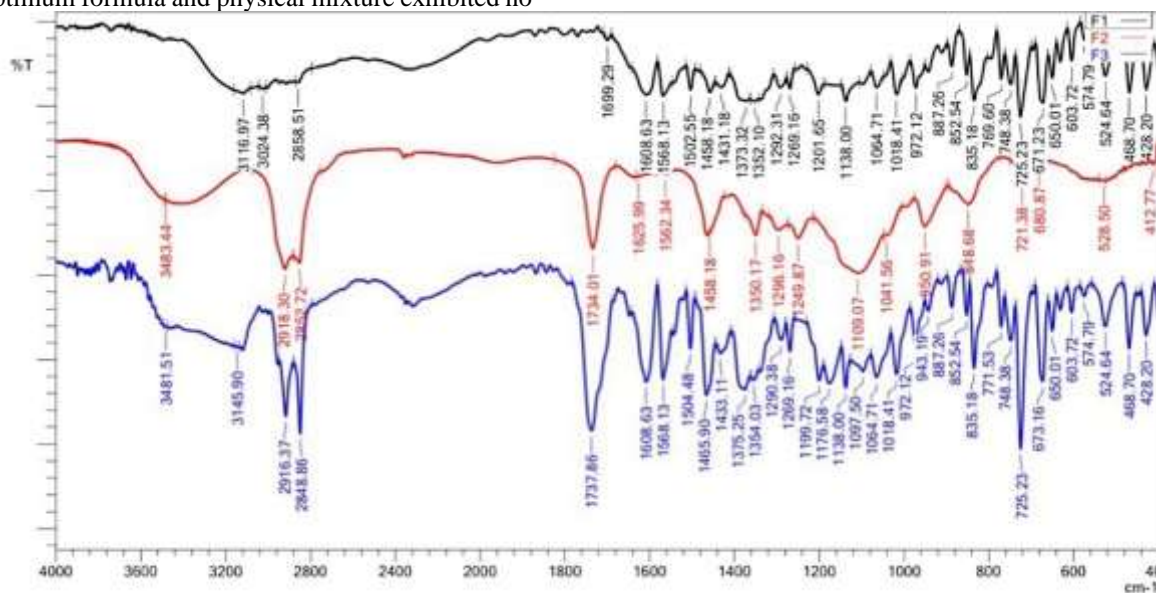
alterations in the drug's structure caused by exposure to rigorous and challenging conditions during the formulation process⁽³³⁾. The FTIR spectra of pure RZB powder revealed distinct peaks, as shown in Table 4.

Table 4. Distinctive peaks of pure Rizatriptan Benzoate⁽³⁴⁾

Functional groups	Peaks (cm ⁻¹)
C-C bending	671.23
C-H bending	887.26
C-C stretching	945.12
C=O stretching of carboxylic acid	1292.31
C-N stretching	1064.71 & 1138.00
C-H bending	1458.18 & 1373.32
C=N stretching	1504.48
N-H bending	1566.20
C=C stretching in aromatic ring	1604.77
C=C bending	2210

Figures 13 illustrate the FTIR analysis of pure RNB, lyophilized form, and physical mixture of the optimum formula, respectively. The RNB optimum formula and physical mixture exhibited no

significant alterations in their functional group regions, with only minor fluctuations in intensity and amplitude⁽³⁵⁾.

**Figure 13. FTIR spectrum of pure RNB (F1), optimum formula (F2), and the physical mixture (F3)****Field emission- scanning electron microscopy (FESEM)**

The size and shape of the nanoparticles were assessed using a field emission scanning electron microscope (FESEM). Figure 14 displays the

pictures of the nanovesicles obtained for the selected formula. The image depicted minuscule particles exhibiting a smooth surface and uniform particle size, distinguished by its small and consistent dimensions^(36,37).

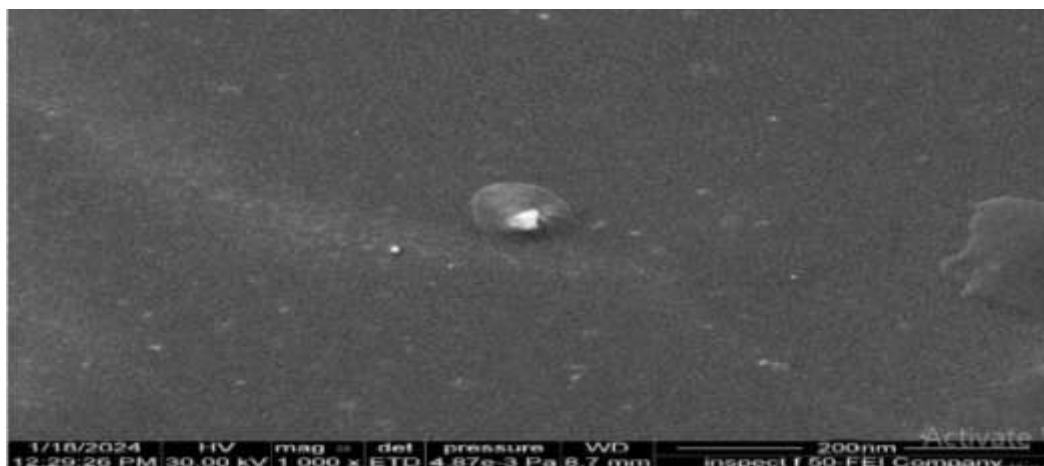


Figure 14. FESEM of the optimum formula

Transmission electron microscopy (TEM)

Transmission electron microscopy (TEM) is a commonly used technique for examining and displaying objects at the nanoscale, providing more resolution than alternative approaches. This advantage is attained by employing a high-energy electron beam with a wavelength that is shorter than that of light. Transmission electron microscopy

(TEM) enables thorough analysis of materials and biological samples at the nanoscale, offering vital information on their structure and shape^(38,39). Figure 15 displays the TEM pictures of the chosen spanlastics optimum formula. The photos display spherical vesicles within the nanometer size range, illustrating the nanostructure vesicular structure.



Figure 15. TEM images of the optimum formula

Differential Scanning Calorimetry Analysis

Differential scanning calorimetry (DSC) allows for the precise measurement of any processes involving the consumption or generation of energy, such as endothermic and exothermic phase changes. DSC is a highly effective method for studying the melting behavior and crystalline state of nanocarriers and raw materials⁽⁴⁰⁾.

DSC analysis of RNB (Figure 16) revealed an endothermic peak at 184.43 °C, which corresponds to its melting point (MP), this finding is consistent with previous investigations⁽⁴¹⁾. Figure 17 displays a thermogram of the lyophilized form of the optimum

formula, the absence of the medication's characteristic melting point peak can be attributed to the even distribution of the drug within the spanlastics nanovesicular system and the dilutional impact of mannitol, this explains the presence of a peak at 163.65°C which belong to mannitol⁽⁴²⁾. DSC analysis of the physical combination (Figure 18) containing RNB and excipients in a 1:1 molar ratio revealed the presence of a distinct melting peak of RNB at 174.54 °C and a melting point of span 60 (60.10°C). However, the intensity of this peak was lower compared to that of pure RNB. The pronounced spike suggests that the substance was in

its crystalline state. The movement of the melting endotherm of the mixture may be caused by the combination of active and excipient ingredients

rather than suggesting any potential incompatibility⁽⁴³⁾.

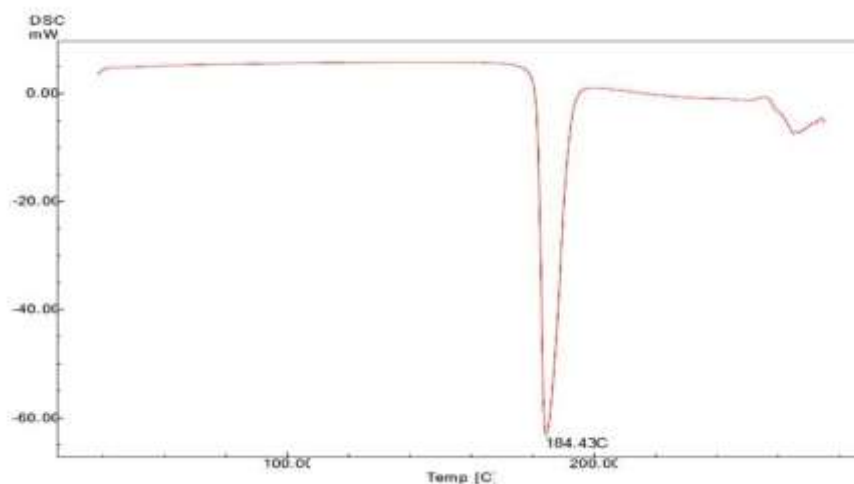


Figure 16. DSC Thermogram of RNB

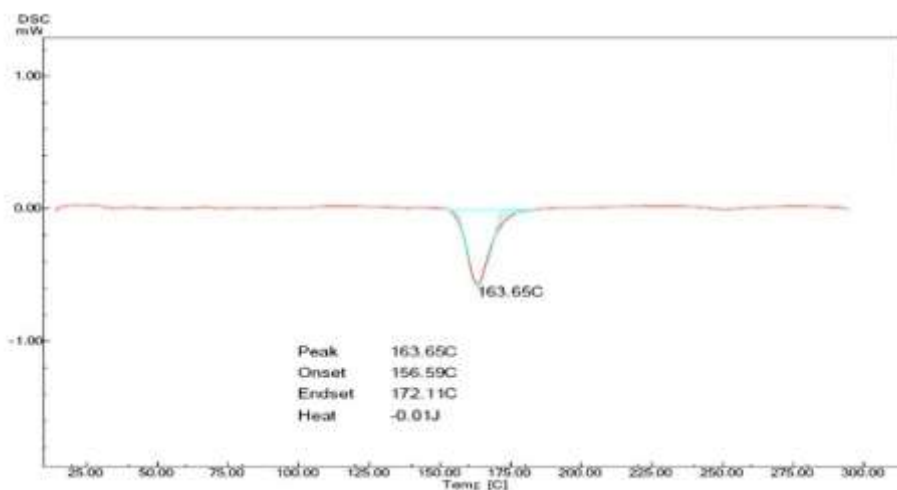


Figure 17. DSC Thermogram of lyophilized form of the optimum formula

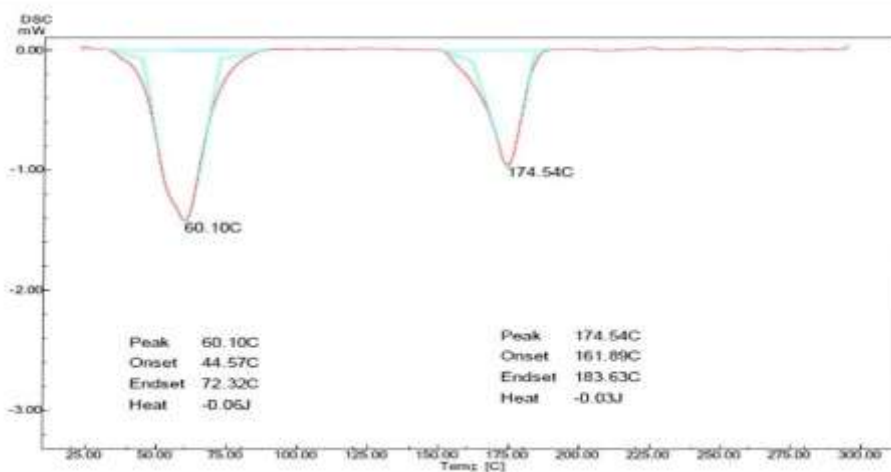


Figure 18. DSC Thermogram of the physical mixture

X-ray Diffraction Analysis

Figure 19 illustrates X-ray diffraction (XRD) patterns used to analyze the crystalline characteristics of the pure drug RNB. The XRD patterns of RNB show prominent diffraction peaks at 2θ values of 20.73° , 25.11° , 44.60° , and 51.25° ⁽⁴⁴⁾. The dispersion of the lyophilized spanlastic formula in (figure 20) had peaks at 2θ values of 20.73° , 25.11° , 44.60° , and 51.25° , became very low in intensity and approximately disappeared. The strongest peaks of 9.8° , 20° , and 25° are attributed to

mannitol, which is utilized as a cryoprotectant in freeze drying ⁽⁴⁵⁾. The physical mixture had distinct peaks of RNB, albeit their intensity was reduced compared to the pure medication. The majority of the prominent peaks associated with the drug RNB have vanished, suggesting a transformation from a crystalline state to a disordered amorphous or molecularly dispersed form. This indicates the potential inclusion of the drug molecule into the spanlastics formula, which could explain the reported high entrapment efficiency ⁽⁴⁶⁾.

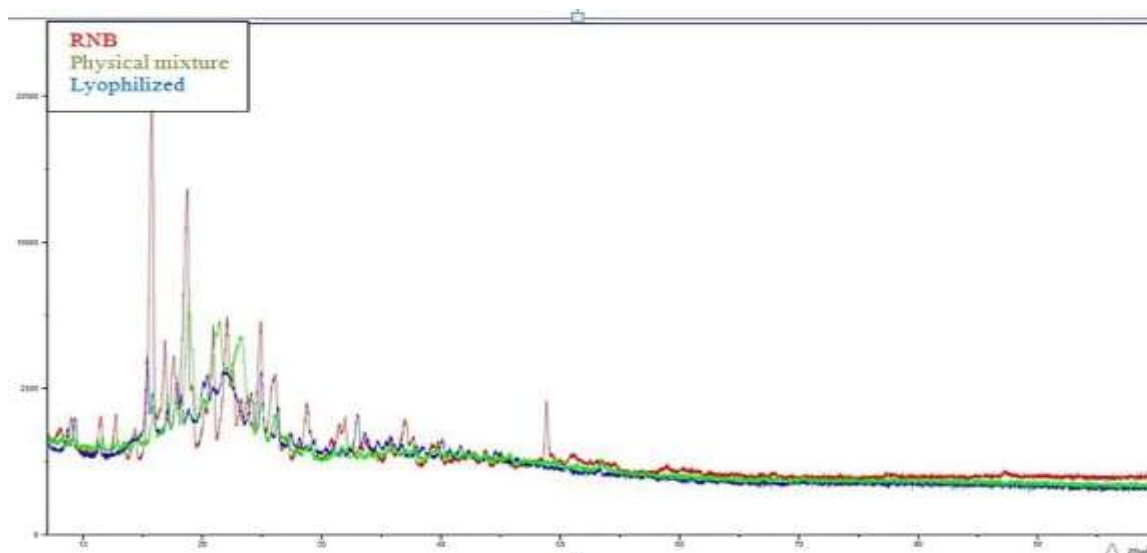


Figure 8 . XRD diffractograms of RNB, lyophilized formula, and physical mixture of the optimized formula

Conclusion

The research findings demonstrate the successful formulation of RNB as a spanlastics formulation. This innovative strategy enhances the ability of medicines to enter the body and provide sustained release for prolonged durations compared to traditional methods. The RNB spanlastics formulation was improved utilizing the Box-Behnken design. The optimized formula exhibits a small vesicle size, lower dispersity Index, and high entrapment, and the soluble amorphous form of the RNB moiety, resulting in a high in vitro release percentage of over 90% during a 6hour period. Additionally, it has a favorable zeta potential, which suggests a well prepared and stable formulation.

Acknowledgment

The authors are grateful to the college of Pharmacy/University of Baghdad for providing the necessary facilities and equipment to conduct and accomplish this study.

Conflicts of Interest

The authors declare that they have no conflicts of interest related to this work.

Funding

This research paper received no specific grant from any funding agency in the public, commercial, or not-for-profit sectors.

Ethics Statements

Since there were no humans or animals involved, no ethical approval was needed for this project.

Author Contribution

Study conception and design: Rajaa A.; data collection: Rajaa A.; analysis and interpretation of results: Rajaa A. and Mowafaq M.; draft manuscript preparation: Rajaa A. and Mowafaq M.; All authors reviewed the results and approved the final version of the manuscript.

References

1. Alhammid SN, Kassab HJ, Hussein, LS, Haiss MA, & Alkufi, Hk. Spanlastics Nanovesicles: An Emerging and Innovative Approach for Drug Delivery. Maaen Journal for Medical Sciences. 2023; 2(3):11-27. <https://doi.org/10.55810/2789-9136.1027>.

2. Chauhan MK, & Verma A. Spanlastics future of drug delivery and argeting . Verma et al. World Journal of Pharmaceutical Research.2017; 6(2): 429-436. <https://doi.org/10.20959/wjpr201712-9726>
3. Ali MM , Shoukri R A, & Yousry C. Thin film hydration versus modified spraying technique to fabricate intranasal spanlastic nanovesicles for rasagiline mesylate brain delivery: Characterization, statistical optimization, and in vivo pharmacokinetic evaluation. Drug Delivery and Translational Research. 2022;13(4):1153–1168. <https://doi.org/10.1007/s13346-022-01285-5>.
4. Salih OS, & Al-Akkam E J. Preparation, In vitro, and Ex vivo Evaluation of Ondansetron Loaded Invasomes for Transdermal Delivery. Iraqi Journal of Pharmaceutical Sciences.2023; 32(3):71–84. <https://doi.org/10.31351/vol32iss3pp71-84>
5. Rajab NA& Jawad MS. Impact of Lipid Type and Ratio in Rizatriptan Benzoate Nanostructured Lipid Carrier. International Journal of Drug Delivery Technology.2023;13(1), 112–119. <https://doi.org/10.25258/ijddt13.1.17>
6. Hadi AS, & Ghareeb MM. Rizatriptan Benzoate Nanoemulsion for Intranasal Drug Delivery: Preparation and Characterization. International Journal of Drug Delivery Technology. 2022; 12 (2), 546–552. <https://doi.org/10.25258/ijddt.12.2.14> .
7. Singh O, Sharma S, Naagar M, Maity MK & Kumar Maity M. Eletriptan as treatment option for acute migraine. In International Journal of Innovations & Research Analysis (IJIRA). 2022; 2(3): 11-26. <https://www.researchgate.net/publication/364657249>
8. Agha OA, Girgis GN. S, El-Sokkary M, & Soliman O.Spanlastic-laden in situ gel as a promising approach for ocular delivery of Levofloxacin: In-vitro characterization, microbiological assessment, corneal permeability and in-vivo study. International Journal of Pharmaceutics. 2023; 11(7): 6. <https://doi.org/10.55810/2789-9136.102>.
9. Abbas IK& Abd-AlHammid, SN. Design, Optimization and Characterization of Self-Nano emulsifying Drug Delivery Systems of Bilastine. Iraqi Journal of Pharmaceutical Sciences. 2023; 32: 164–176. <https://doi.org/10.31351/vol32issSuppl.pp164-176> .
10. Ali SK & Al-Akkam E J. Bilosomes as Soft Nanovesicular Carriers for Ropinirole Hydrochloride: Preparation and In- vitro Characterization. Iraqi Journal of Pharmaceutical Sciences .2023 ;32: 177–187. <https://doi.org/10.31351/vol32issSuppl.pp177-187> .
11. Salih Z T & Al- Gawhari F Improvement of Entrapment and Ocular Permeability of Ganciclovir Nano structured Lipid Carriers Using Various Conditions of Preparations. International Journal of Drug Delivery Technology. 2023; 13(1): 341–346. <http://dx.doi.org/10.25258/ijddt.13.1.55>.
12. Mahal R.K& Al-Gawhari F . Design, Development and Optimization of Solid Lipid Nanoparticles for Ocular Delivery of an Antifungal Agent. IJDDT. 2023; 13(1: 327-339. DOI: 10.25258 /ijddt.12.4.36
13. Salih OS, & Al-Akkam EJ. Preparation, In vitro, and Ex vivo Evaluation of Odansetron Loaded Invasomes for Transdermal Delivery. Iraqi Journal of Pharmaceutical Science. 2023; 32(3): 71–84. <https://doi.org/10.31351/vol32iss3pp71-84> .
14. Mahmood AA, &Alhammid SNA. Preparation and Ex-Vivo Evaluation of Stabilized Cefdinir Nano suspension. Pakistan Journal of Medical and Health Sciences. 2022; 16(12): 789–794. <https://doi.org/10.53350/pjmhs20221612789> .
15. Rashid AM &Abd-Alhammid SN. Formulation and characterization of itraconazole as nano suspension dosage form for enhancement of solubility. Iraqi Journal of Pharmaceutical Sciences. 2019; 28(2): 124–133. <https://doi.org/10.31351/vol28iss2pp124-133>.
16. Saad A & Sabri L. Study The Variables Affecting Formulation of Ethylcellulose -based Micro sponges loaded with Clobetasol. Iraqi Journal of Pharmaceutical Sciences. 2023; 32: 225–234. <https://doi.org/10.31351/vol32issSuppl.pp225-234>.
17. Atiyah Altameemi KK, & Abd-Alhammid SN. Anastrozole Nanoparticles for Transdermal Delivery through Microneedles: Preparation and Evaluation. Journal of Pharmaceutical Negative Results. 2022; 13(3): 974–980. <https://doi.org/10.47750/pnr.2022.13.03.152>.
18. Salih OS, Jasim E, Salih OS& Al-Akkam E J. Review Article Invasomes as a Novel Delivery Carrier for Transdermal Delivery: Review Article Citation. In Medicin Pharmaceutical Sciences. 2022; 2(3) :23-29. <https://www.researchgate.net/publication/371951443> .
19. Tamer MA, & Kassab HJ. The development of a brain targeted mucoadhesive amisulpride loaded nanostructured lipid carrie. Farmacia 2023; 71(5): 1032–1044. <https://doi.org/10.31925/farmacia.2023.5.18>
20. Talal Sulaiman, & Rajab NA. Soluplus and solutol HS-15olmesartan medoxomil nanomicelle based oral fast dissolving film; in vitro and in vivo characterization. Faramacia. 2024; 72, 4. <https://doi.org/10.31925/farmacia.2024.4.7>.

21. Jassim BM, & Al-Khedairy EBH. Formulation and in vitro /in vivo Evaluation of Silymarin Solid Dispersion-Based Topical Gel for Wound Healing. *Iraqi Journal of Pharmaceutical Sciences*. 2023; 32: 42–53. <https://doi.org/10.31351/vol32issSuppl.pp42-53>
22. Bhardwaj P, Tripathi P, Pandey S, Chaurasia D, & Ramchandra P P. Tailored Non-ionic Surfactant Vesicles of Cyclosporine for the Treatment of Psoriasis: Formulation, Ex-Vivo and In-Vivo investigation -Application of Box-Behnken Design. *Advanced Materials Science and Technology*. 2023; 5(2): 0–0. <http://dx.doi.org/10.37155/2717-526X-0502-2>
23. Owodeha-Ashaka K, Ilomuanya MO, Iyire A. Evaluation of sonication on stability-indicating properties of optimized pilocarpine hydrochloride-loaded niosomes in ocular drug delivery. *Progress in Biomaterials*. 2021;10(3):207-220. doi: 10.1007/s40204-021-00167-2.
24. Iskandarsyah I, Masrijal CDP, &Harmita H. Effects of sonication on size distribution and entrapment of lynestrenol transfersome. *International Journal of Applied Pharmaceutics*. 2020; 12(1): 245–247. <https://doi.org/10.22159/ijap.2020.v12s1.FF053>
25. Chen X, & Wang T. Preparation and characterization of atrazine-loaded biodegradable PLGA nanospheres. *Journal of Integrative Agriculture*. 2019 ;18(5), 1035–1041. [https://doi.org/10.1016/S2095-3119\(19\)62613-4](https://doi.org/10.1016/S2095-3119(19)62613-4)
26. Jassem NA, &Alhammad SNA. Ex vivo permeability study and in vitro solubility characterization of oral Canagliflozin self-nanomicellizing solid dispersion using Soluplus® as a nanocarrier. *Acta Marisiensis - Seria Medica* .2024 ;70(2), 42–49. <https://doi.org/10.2478/amma-2024-0011>
27. Badria F &Mazye E. Formulation of nanospanlastics as a promising approach for improving the topical delivery of a natural leukotriene inhibitor (3-acetyl-11-keto- β -boswellic acid): Statistical optimization, in vitro characterization, and ex vivo permeation study. *Drug Design, Development and Therapy*. 2020; 14, 3697–3721. <https://doi.org/10.2147/DDDT.S265167>
28. Zeng L, Xin X, & Zhang Y. Development and characterization of promising Cremophor EL-stabilized o/w nanoemulsions containing short-chain alcohols as a cosurfactant. *RSC Advances*. 2017; 7(32), 19815–19827. <http://doi.org/10.1039/C6RA27096D>
29. Sailaja AK. Formulation and Evaluation of Aspirin Nanosuspension Using Probe Sonication Method. *International Journal of Clinical Case Reports and Reviews*. 2023; 14(1):01–04. <https://doi.org/10.31579/2690-4861/314>
30. Mazyed EA, Helal DA, Elkhoudary MM, Abd Elhameed AG & Yasser M. Formulation and optimization of nanospanlastics for improving the bioavailability of green tea epigallocatechin gallate. *Pharmaceuticals*. 2021; 14(1): 1–30. <https://doi.org/10.3390/ph14010068>
31. Badria FA, Fayed HA, Ibraheem AK. Formulation of sodium valproate nanospanlastics as a promising approach for drug repurposing in the treatment of androgenic alopecia. *Pharmaceutics*. 2020;12(9):1–27. <https://doi.org/10.3390/pharmaceutics12090866>
32. Girotra P, Singh SK. Multivariate Optimization of Rizatriptan Benzoate-Loaded Solid Lipid Nanoparticles for Brain Targeting and Migraine Management. *AAPS PharmSciTech*. 2017; 18(2):517-528. doi: 10.1208/s12249-016-0532-0.
33. Nair AB, Shah J, Jacob S, Al-Dhubiab BE, Patel V, Sreeharsha N. Development of mucoadhesive buccal film for rizatriptan: In vitro and in vivo evaluation. *Pharmaceutics*. 2021;13(5) :7-12. <https://doi.org/10.3390/pharmaceutics13050728>
34. Salve P, Bali N. Fabrication and optimization of buccal film comprising rizatriptan benzoate loaded solid lipid nanoparticles for improved ex vivo permeation. 2019; 9:636–48. <https://doi.org/10.1016/j.matpr.2015.10.067>
35. Khan MI, Madni A, Ahmad S, Mahmood MA, Rehman M, Ashfaq M. Formulation design and characterization of a non-ionic surfactant based vesicular system for the sustained delivery of a new chondroprotective agent. *Brazilian Journal of Pharmaceutical Sciences*.2015;51: 607-615. <https://doi.org/10.1590/S1984-8250201500300012>
36. Yadav SK, Mishra S, Mishra B. Eudragit-based nanosuspension of poorly water-soluble drug: formulation and in vitro-in vivo evaluation. *American Association of Pharmaceutical Scientists* 2012;13(4):1031–44.
37. Tamer, MA, & Kassab HJ. Optimizing Intranasal Amisulpride Loaded Nanostructured Lipid Carriers: Formulation, Development, and Characterization Parameters. *Pharmaceutical Nanotechnology*.2024; 12:1-15. <https://doi.org/10.2174/0122117385301604240226111533>
38. Abdullah T&Al-Kinani K. Propranolol nanoemulgel: Preparation, in-vitro and ex-vivo characterization for a potential local hemangioma therapy. *Pharmacia*. 2024; 71: 1–12. <https://doi.org/10.3897/pharmacia.71.e115330>

39. Neamah MJ, & Al-Akkam, EJM. Preparation and characterization of vemurafenib microemulsion based hydrogel using surface active ionic liquid. *Pharmacia*. 2024;71:1-9. <https://doi.org/10.3897/pharmacia.71.e111178>
40. Soliman MA, Ibrahim HK, Nour SA. Diacerein solid dispersion loaded tablets for minimization of drug adverse effects: statistical design, formulation, in vitro, and in vivo evaluation. *Pharmaceutical Development and Technology*. 2021; 16; 26(3):302-15. <https://doi.org/10.1080/10837450.2020.1869982>
41. Rajab NA & Jawad MS. Preparation and Evaluation of Rizatriptan Benzoate Loaded Nano structured Lipid Carrier Using Different Surfactant/Co-Surfactant Systems. *International Journal of Drug Delivery Technology*. 2023; 13(1): 120-126. <https://doi.org/10.25258/ijddt.13.1.18>
42. Hana YK, Faudoneb SN, Zittob G, Bonafedea SL, Rosascoa MA, Segalla AI. Physicochemical Characterization of Physical Mixture and Solid Dispersion of Diclofenac Potassium with Mannitol. *Journal of Applied Pharmaceutical Science*. 2017;7(1):204-8. <https://dx.doi.org/10.7324/JAPS.2017.70130>
43. Frank D, Schenck L, Koynov A, Su Y, Li Y, Variankaval N. Optimizing solvent selection and processing conditions to generate high bulk-density, coprecipitated amorphous dispersions of posaconazole. *Pharmaceutics*. 2021;13(12): 17-20. <https://doi.org/10.3390/pharmaceutics13122017>
44. Chaudhari P, Kolhe S & More, D. Formulation Development Studies of Rizatriptan Benzoate Fast Disintegrating Tablet. *Research journal of pharmaceutical biological and chemical sciences*. 2011; 4(6) :176-186.
45. Ahmed EM, Nabil SR, Faten F, Mohamed NS. Bilosomes as a novel carrier for the cutaneous delivery for dapsone as a potential treatment of acne: Preparation, characterization and in-vivo skin deposition. *J Liposome Res*. 2020; 30(1):1-11. <https://doi.org/10.1080/08982104.2019.1577256>
46. Singh A, Ubrane R, Prasad P, Ramteke S. Preparation and Characterization of Rizatriptan Benzoate Loaded Solid Lipid Nanoparticles for Brain Targeting. *Materials Today: Proceedings*. 2015;2(9):4521-43. <https://doi.org/10.1016/j.matpr.2015.10.067>

تصميم وتطوير وتحسين السبائلاستيك لتوصيل دواء الريزاتريبتان بنزوات

رجاء عباس دهش^١، و موفق محمد غريب^٢

^١ وزارة الصحة، بغداد، العراق.

^٢ فرع الصيدلانيات، كلية الصيدلة، جامعة بغداد، بغداد، العراق.

الخلاصة

السبائلاستيك هو نوع جديد من حاملات الحويصلات النانوية المرنة التي تتكون من منشط الحافة وخافض غير ابوني للتوتر السطحي، ويمكن اعطاء الادوية الكارهة للماء او المحبة للماء، تعمل السبائلاستيك على تعزيز قدرة الادوية على دخول الجسم وتوفير تحرر مستمر للدواء على فترات طويلة. السبائلاستيك تمتلك درجة عالية من المطاطية والمرونة، مما يمكنها من تحسين نقل الادوية من خلال طرق الاعطاء المختلفة. تم استخدام بوكس بينكن دز اين لانشاء علاقة بين المتغيرات المستقلة (كمية سبان ٦٠، كمية الكريموفور ٤٠، ووقت الصوتنة) والمتغيرات التابعة (حجم الجسيمات، مؤشر التشتت وكفاءة الحصر) تم تطوير تركيبات السبائلاستيك باستخدام عملية حقن الايثانول. تم تحليل الجسيمات من اجل تحديد الصيغة المثالية التي تحتوي على حجم جسيمات من اجل تحديد الصيغة المثالية التي تحتوي على حجم جسيم صغير واقل مؤشر تشتت وكفاءة حصر عالية. خضعت الصيغة المثالية لفحوصات اضافية مثل جهد الزيت وتحرر الدواء في المختبر، التحليل الطيفي بالأشعة تحت الحمراء، والمسح المجهر الإلكتروني، واستخدام حنود المسحوق بالأشعة السينية. اظهرت الصيغة المثالية حجم جسيم قدره (84.98 ± 2.36) ومؤشر تشتت (0.1993 ± 0.045) وكفاءة حصر $(53.69 \pm 1.08 \%)$ ، هناك اختلاف قليل بين الصيغة المقترضة والصيغة الفعلية، جهد الزيت (22.73 ± 0.74) وكان تحرر الدواء مستمرا (88.5 ± 2.3) خلال ٦ ساعات. تحليل التوافق اظهر ان الريزاتريبتان بنزوات متوافق مع المواد المضادة ووجد جزء من الدواء في حالة غير متبلورة وكان شكل الحويصلة شبه كروية. باختصار اظهرت النتائج ان السبائلاستيك لديها القدرة للعمل كناقلات لتوصيل دواء الريزاتريبتان بنزوات.

الكلمات المفتاحية: كريموفور ٤٠، ريزاتريبتان بنزوات، حويصلات، سبان ٦٠، سبائلاستيك.